Supplementary Information

Barbiturate End-Capped Non-Fullerene Acceptors for Organic Photovoltaics: Tuning Acceptor Energetics to Suppress Geminate Recombination Losses

Ching-Hong Tan[a], Jeffrey Gorman[b], Andrew Wadsworth[a], Sarah Holliday*[c], Selvam Subramaniyan[d], Samson A. Jenekhe[d], Derya Baran[e], Iain McCulloch[a, e] James R. Durrant*[a]

a. *Department of Chemistry and Centre for Plastic Electronics, Imperial College London SW7 2AZ London, United Kingdom.*

b. *Cavendish Laboratory, University of Cambridge, CB2 1TN, United Kingdom.*

c. *Department of Materials Science and Engineering, University of Washington, Seattle, WA 98195, United States of America.*

d. *Departments of Chemical Engineering and Chemistry, University of Washington, Seattle, Washington 98195-1750, United States*

e. *Physical Sciences and Engineering Division, KAUST Solar Centre (KSC), King Abdullah University of Science and Technology (KAUST), Thuwal, 23955-6900, Kingdom of Saudi Arabia.*

smgh@uw.edu and j.durrant@imperial.ac.uk

	Contents	**Figure/Table**
1.	Experimental procedures and synthetic procedure for FTB and FTTB	Figure S1-S4
2.	Minimum energy conformation calculation of FTB and FTTB molecules using Gaussian (B3LYP/6-13G*)	Figure S5
3.	UV-vis absorption measurements and CV of neat FTB, FTTB and PSEHTT films	Table S1/Figure S6-S8
4.	Device optimization of PSEHTT:acceptor systems	Table S2-S3
5.	XRD measurements of neat FTB, FTTB, PSEHTT with and without annealing	Figure S9
6.	XRD measurements and UV-vis spectra of the blend films with and without annealing	Figure S10
7.	PL measurement of neat PSEHTT, FTB and FTTB and the blend films excited at 650 and 460 nm	Figure S11 and S 12
8.	Electron and hole mobility measurement and calculation of PSEHTT:FTB and PSEHTT:FTTB devices	Figure S13-S14/Table S4
9.	TA spectra of neat PSEHTT, FTB and FTTB films	Figure S15
10.	Excitation dependence decays of FTB:PSEHTT and FTTB:PSEHTT blends	Figure S16

Experimental Procedures

OSC Device Fabrication and Characterisation

Solar cells were fabricated on pre-patterned used as received ITO-coated glass substrates. Prior to spin-coating deposition, substrates were cleaned using: detergent, deionized water, acetone, and isopropanol sequentially in sonication and treated with oxygen plasma for around 8 min. A ZnO-precursor solution (219.5 mg zinc acetate dehydrate precursor in 2 mL 2-methoxyethanol and 60 µL monoethanolamine) was spun coated on the substrates giving a thickness of around 30nm followed by annealing at 150°C for 20 min. Devices were transferred to a N_2-filled glovebox where the optimized blend layers (encompassing of 1:2 ratio donor:acceptor in 10 mg/mL chlorobenzene solution stirred for about 24 hours at 60°C) of around 70-80 nm thickness were deposited by spin coating between 3000-5000 rpm for 1 min on the substrates. 10 nm MoO_3 and 100 nm Ag layers were consecutively deposited on the substrates in an evaporation chamber at $2x10^{-6}$mbar through a shadow mask of 0.045 cm^2 active area. Completed devices were kept in glovebox conditions. J-V curves were recorded using a Xenon lamp set at AM1.5G and 1 sun (100 $mWcm^{-2}$) illumination from Oriel Instruments and calibrated using a Si reference cell with a Keithley 2400 source meter. External quantum efficiency (EQE) was measured with a 100W tungsten-halogen lamp (Bentham IL1 with Bentham 605 stabilised current power supply) illumination connected to a monochromator with an automated stepper motor. Photon flux was calibrated to a Si reference cell using a Keithley 2400 source meter for spectra mismatch correction.

Material Characterisation

^1H and ^{13}C NMR spectra were recorded on a Bruker AV-400 spectrometer at 298 K, reported in ppm. UV-vis spectra were obtained using a Shimadzu UV-Vis Spectrophotometer UV-26000. Mass spectrometry was carried out with a Micromass matrix assisted laser desorption ionisation with time-of-flight (MALDI-ToF). DSC thermograms were recorded on a TA Instruments DSC Q20 at a heating rate of 5 °C min^{-1}, samples were drop-cast from $CHCl_3$ solutions onto glass slides to allow solvent to evaporate and then these samples were transferred to DSC pans. Specular X-Ray Diffraction was measured on a PANalytical X'Pert PRO MRD diffractometer with a Ni-filtered Cu-Kα1 beam (λ= 0.154184 nm) and X'Celerator detector (current 40 mA, accelerating voltage 40 kV). Cyclic voltammetry (CV) was measured on an Autolab PGSTAT101 potentiostat with a three-electrode setup using Ag/AgCl reference electrode, Pt counter-electrode, and with thin films spin coated on ITO as the working electrode. A 0.1 M tetrabutylammonium hexafluorophosphate in dry acetonitrile electrolyte was used. Outputs were referenced against a ferrocene electrolyte with Pt working electrode. HOMO levels were calculated using: HOMO (eV) = $E_{red} - E_{Fc} + 4.8$, where E_{red} is the onset of reduction and E_{Fc} is the half-wave potential of the ferrocene reference.

Photoluminescence (PL) and fs-transient absorption (TA) spectroscopies

Films for *fs*-TAS and PL were coated on glass with the same active layer processing conditions as optimised photovoltaic devices.

PL spectra employing excitation wavelengths of 460 and 650 nm were recorded with a steady state spectrofluorometer (Horiba Jobin Yvon, Spex Fluoromax 1).

fs-TAS measurement was carried out using a 800 nm (1 kHz, 90 fs) laser-pulse with a Solstice (Newport Corporation) Ti:sapphire regenerative amplifier. Part of the laser pulse, of which spot size is 0.5mm, was used as the 650 nm, 2 μJ cm^{-2} pump-laser with a TOPAS-Prime (Light conversion) optical parametric amplifier. The other laser output generated the probe light in the infrared continuum (850-1400 nm) with a sapphire crystal. Spectra and decays were obtained by a HELIOS transient absorption spectrometer (450–1450 nm) and decays to 6 ns. Films were measured in an N_2 atmosphere and blend spectra was deconvoluted by fitting the singlet PSEHTT exciton ($S_{exciton}$) and blend polaron ($S_{polaron}$) at 6 ns to the blend spectra using:

$$\Delta OD = D * S_{exciton}(1300\,nm) + P * P_{polaron}(1050\,nm)$$

where D and P are linear coefficients of exciton and polaron respective in the blend spectra. $S_{exciton}$ and $P_{polaron}$ are the exciton and polaron spectra of PSEHTT donor and blend.

Charge Mobility

Electron-only devices were fabricated in ITO/ZnO/Active Layer/Ca/Al and hole-only in ITO/PEDOT:PSS/Active Layer/MoO_3/Ag architectures. Device J-V curves were measured under dark conditions between -8 V to 8 V at slow 0.05 V step changes using a Keithley 2400 source meter. Blend mobility was calculated using the SCLC expression described by the Mott-Gurney law were the j-V follows the space-charge regime:

$$J = \frac{9}{8}\varepsilon_0\varepsilon_r\mu\frac{V^2}{L^3}$$

Where ε_0 is vacuum permittivity, ε_r = 3, μ is the carrier mobility, L is active layer thickness, and V is the applied voltage.

Synthetic Procedure

2,7-Bis(4,4,5,5-tetramethyl-1,3,2-dioxaborolan-2-yl)-9,9-dioctylfluorene (**1**) was synthesized by according to literature procedures.[1, 2] All other reagents and solvents were purchased from commercial sources (Sigma-Aldrich, Alfa Aesar, Acros Organics or TCI) and used as received. Reactions were carried out in an inert argon atmosphere using conventional Schlenk line techniques.

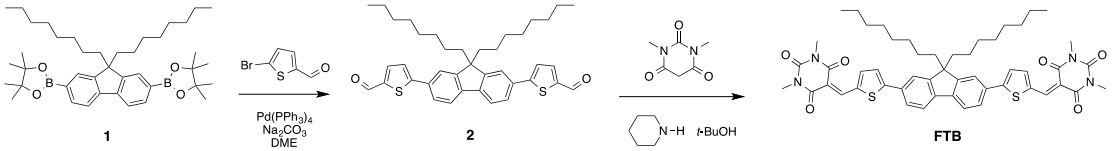

Scheme S1: Synthesis of FTB.

5,5'-(9,9-dioctyl-9H-fluorene-2,7-diyl)bis(thiophene-2-carbaldehyde) (**2**) was synthesised according to a modified procedure[3]**:** A solution of 2,7-bis(4,4,5,5-tetramethyl-1,3,2-dioxaborolan-2-yl)-9,9-dioctylfluorene (2.50 g, 3.89 mmol) (**1**) in dimethoxyethane (20 cm^3) was purged with argon gas for 1 hr before the addition of 5-bromo-2-thiophenecarboxaldehyde (1.39 cm^3, 11.7 mmol) and $Pd(PPh_3)_4$ (0.22 g, 0.19 mmol). After further purging this solution with argon gas for 1 hr, a pre-purged solution of aq. Na_2CO_3 (2M, 12 cm^3) was

added and the mixture was heated overnight at 90 °C. The reaction was then cooled to room temperature and extracted with CH_2Cl_2, dried over $MgSO_4$ and the solvent was removed *in vacuo*. Column chromatography (silica gel, CH_2Cl_2) followed by recrystallization from CH_2Cl_2/methanol gave **2** as a yellow solid (1.8 g, 76%). ^{1}H NMR (400 MHz, $CDCl_3$) δ: 9.91 (s, 2H), 7.78-7.75 (m, 4H), 7.70 (dd, J = 8.2 Hz, 1.8 Hz, 2H), 7.64 (d, J = 1.6 Hz, 2H), 7.49 (d, J = 3.9 Hz, 2H), 2.05-1.97 (m, 4H), 1.15-1.02 (m, 20H), 0.78 (t, J = 7 Hz, 6H), 0.70-0.61 (m, 4H). ^{13}C NMR (101 MHz, $CDCl_3$) δ: 182.68, 154.78, 152.27, 142.27, 141.64, 137.40, 134.59, 132.43, 125.73, 124.05, 120.79, 120.72, 55.57, 40.21, 31.74, 29.88, 29.14, 23.77, 22.57, 14.03.

FTB was synthesised according to a modified procedure[4]: 1,3-dimethylbarbituric acid (0.17 g, 1.08 mmol) and **2** (0.22 g, 0.36 mmol) were dissolved in tert-butyl alcohol (15 cm^3) with gentle heating. 1 drop piperidine was added and the solution was stirred overnight at 85 °C. After cooling to room temperature, the crude product was purified by column chromatography on silica gel (CH_2Cl_2) followed by recrystallization from CH_2Cl_2/ethanol, yielding **FTB** as a red solid (0.24g, 74%). ^{1}H NMR (400 MHz, Chloroform-*d*) δ 8.70 (s, 2H), 7.90 (d, J = 4.4 Hz, 2H), 7.85 (dd, J = 8.1, 1.5 Hz, 2H), 7.81 – 7.73 (m, 4H), 7.61 (d, J = 4.3 Hz, 2H), 3.46 (d, J = 15.4 Hz, 12H), 2.21 – 1.94 (m, 4H), 1.24 – 0.94 (m, 20H), 0.76 (t, J = 7.0 Hz, 6H), 0.63 (tt, J = 11.3, 6.5 Hz, 4H). ^{13}C NMR (101 MHz, $CDCl_3$) δ: 162.80, 162.19, 161.12, 152.42, 151.44, 148.72, 147.20. 142.20, 136.14, 132.69, 126.18, 124.78, 120.89, 109.23, 55.86, 40.29, 31.74, 29.98, 29.21, 29.17, 28.95, 28.20, 23.79, 22.57, 14.04. MS (MALDI-ToF): m/z calculated for $C_{51}H_{58}N_4O_6S_2$: 886.38; m/z found 887.9 $(M + 1)^+$.

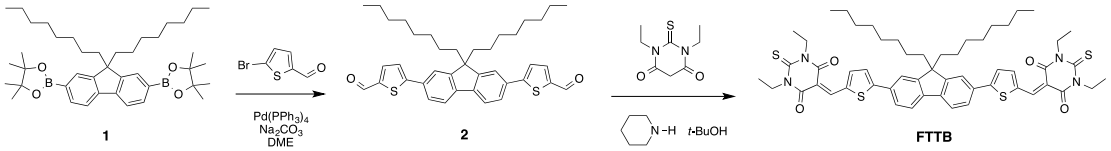

Scheme S2: Synthesis of FTTB.

FTTB was synthesised according to a modified procedure[5]: 1,3-diethyl-2-thiobarbituric acid (0.24 g, 1.22 mmol) and **2** (0.25 g, 0.41 mmol) were dissolved in tert-butyl alcohol (20 cm^3) with gentle heating. 1 drop piperidine was added and the solution was stirred overnight at 85 °C. After cooling to room temperature, the crude product was purified by column chromatography on silica gel (CH_2Cl_2) followed by recrystallization from CH_2Cl_2/ethanol, yielding FTTB as a red solid (0.32 g, 80%). ^{1}H NMR (400 MHz, $CDCl_3$) δ 8.70 (s, 2H), 7.92 (d, J = 4.1 Hz, 2H), 7.87 (dd, J = 8.0, 1.5 Hz, 2H), 7.82 – 7.74 (m, 4H), 7.64 (d, J = 4.2 Hz, 2H), 4.63 (dq, J = 21.1, 6.9 Hz, 8H), 2.19 – 2.05 (m, 4H), 1.36 (dt, J = 22.1, 6.9 Hz, 12H), 1.21 – 1.00 (m, 20H), 0.76 (t, J = 6.9 Hz, 6H), 0.70 – 0.57 (m, 4H). ^{13}C NMR (101 MHz, $CDCl_3$) δ 161.93, 160.01, 152.47, 149.64, 147.44, 142.33, 126.37, 125.11, 120.96, 110.19, 77.33, 77.22, 77.02, 76.70, 55.88, 44.03, 43.18, 40.28, 31.72, 29.86, 29.16, 23.80, 22.56, 12.57.

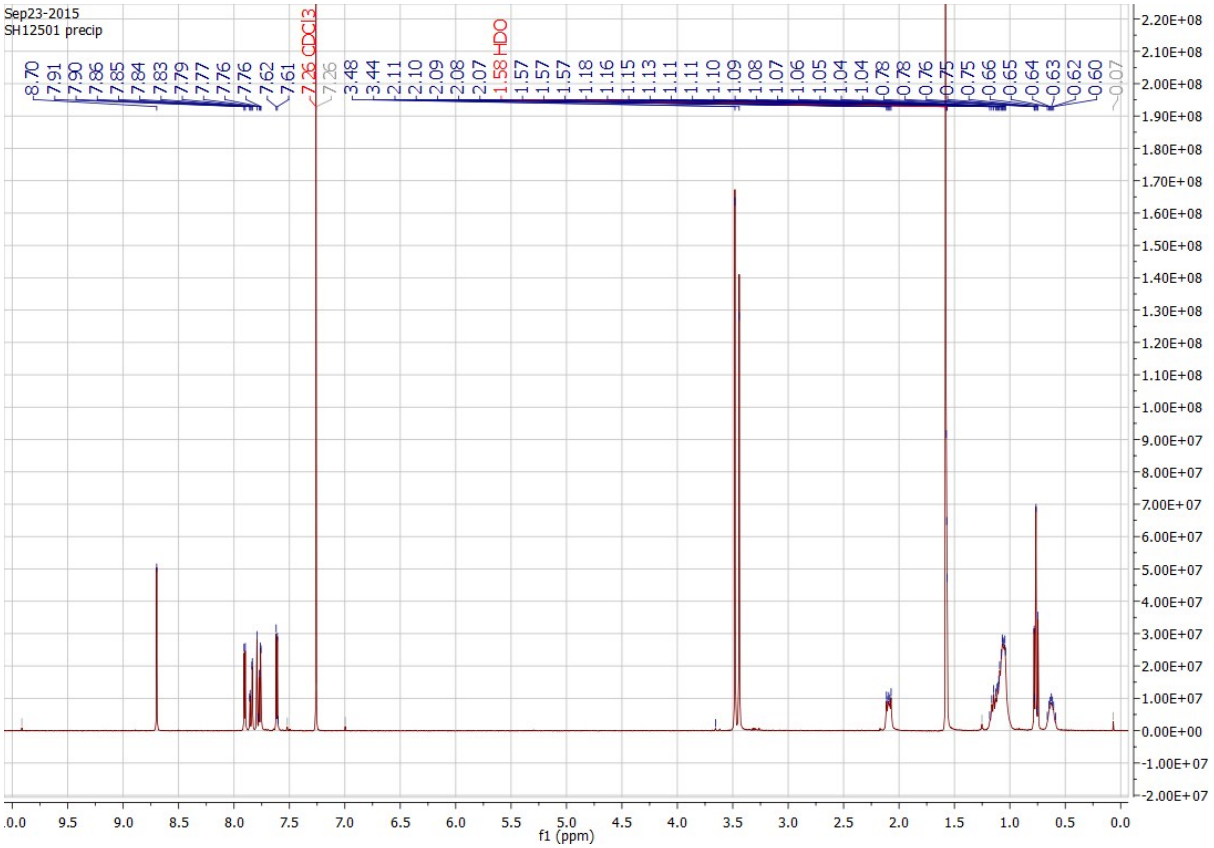

Figure S1: ^{1}H-NMR of FTB in $CDCl_3$.

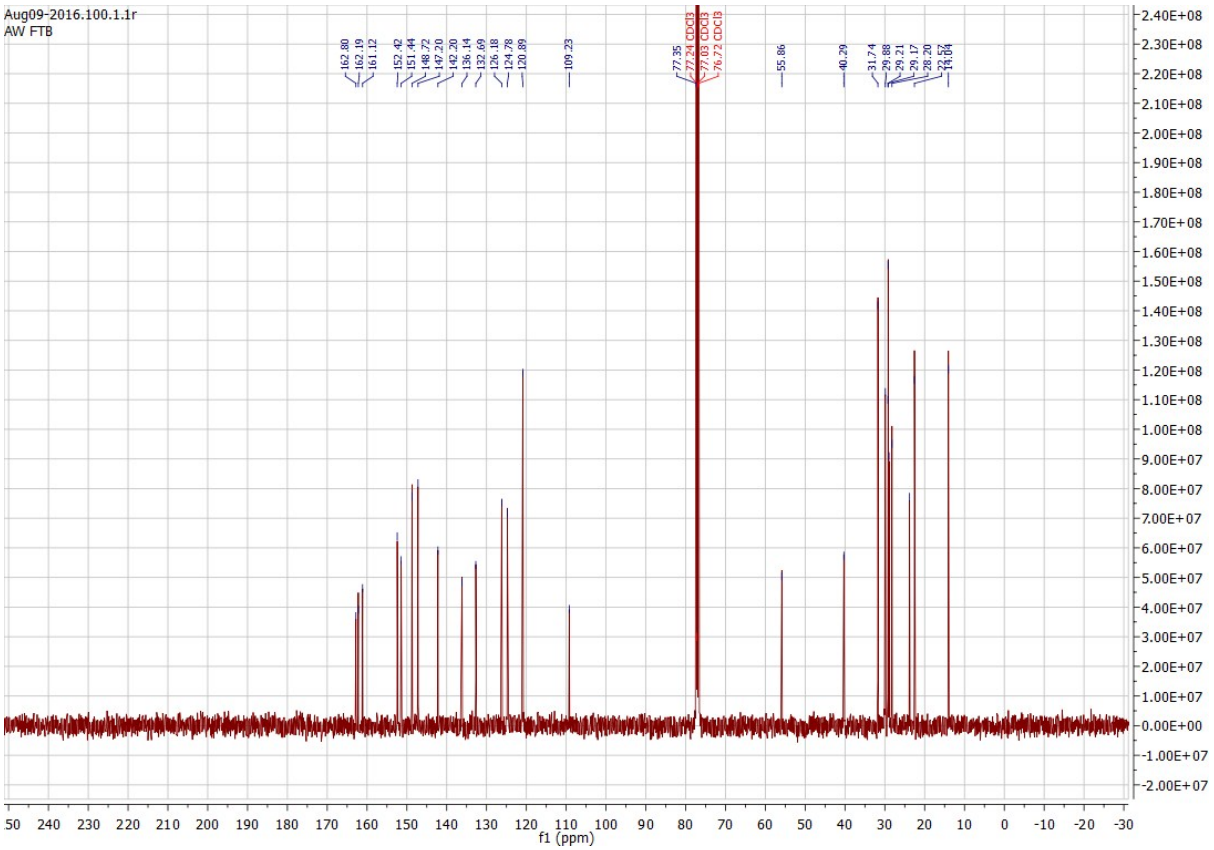

Figure S2: ^{13}C-NMR of FTB in $CDCl_3$.

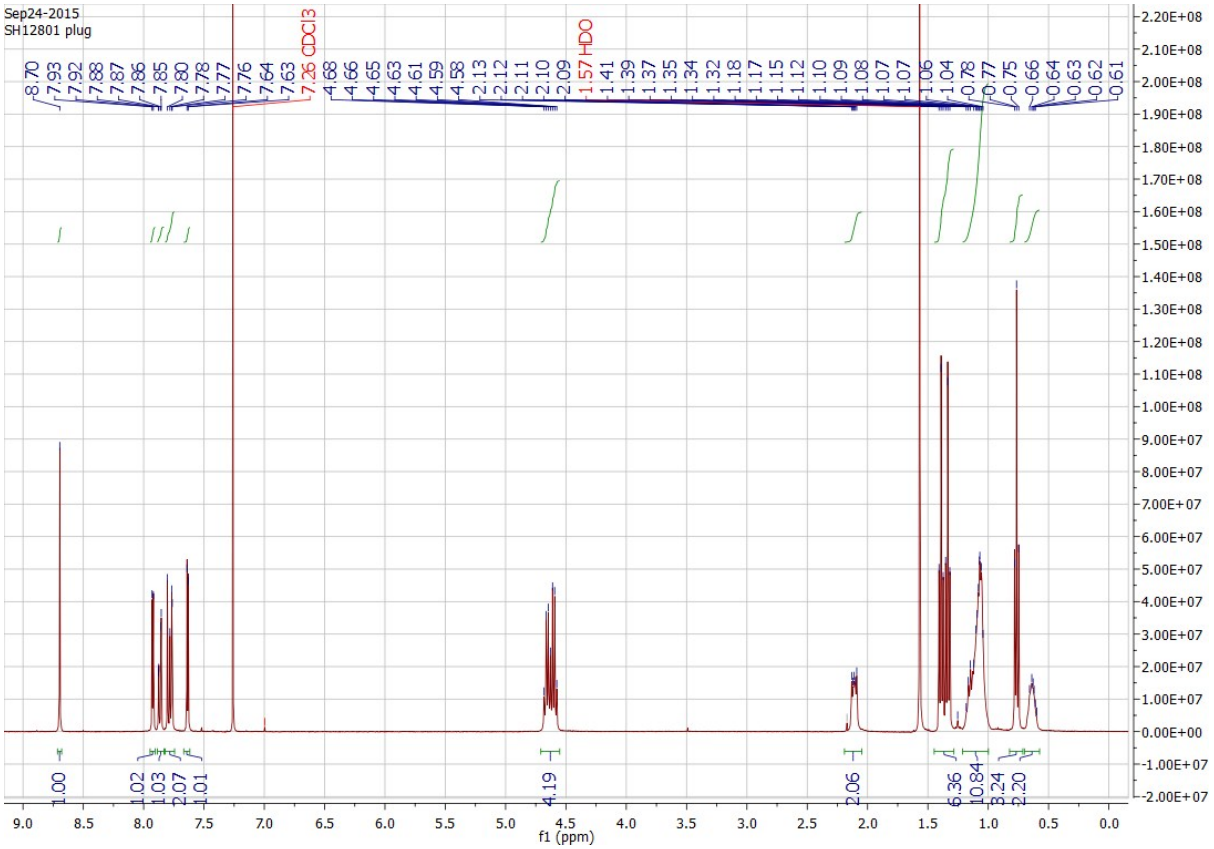

Figure S3: ^{1}H-NMR of FTTB in $CDCl_3$.

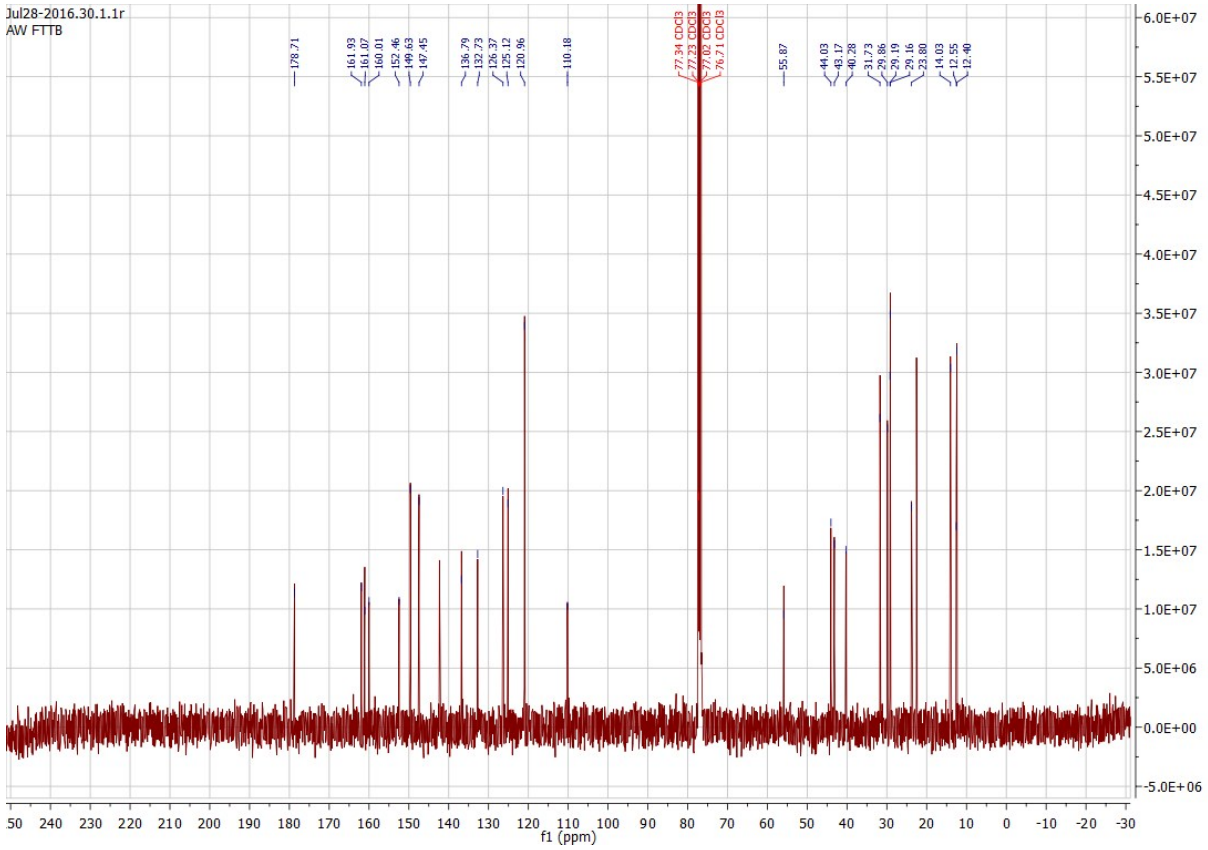

Figure S4: ^{13}C-NMR of FTTB in $CDCl_3$

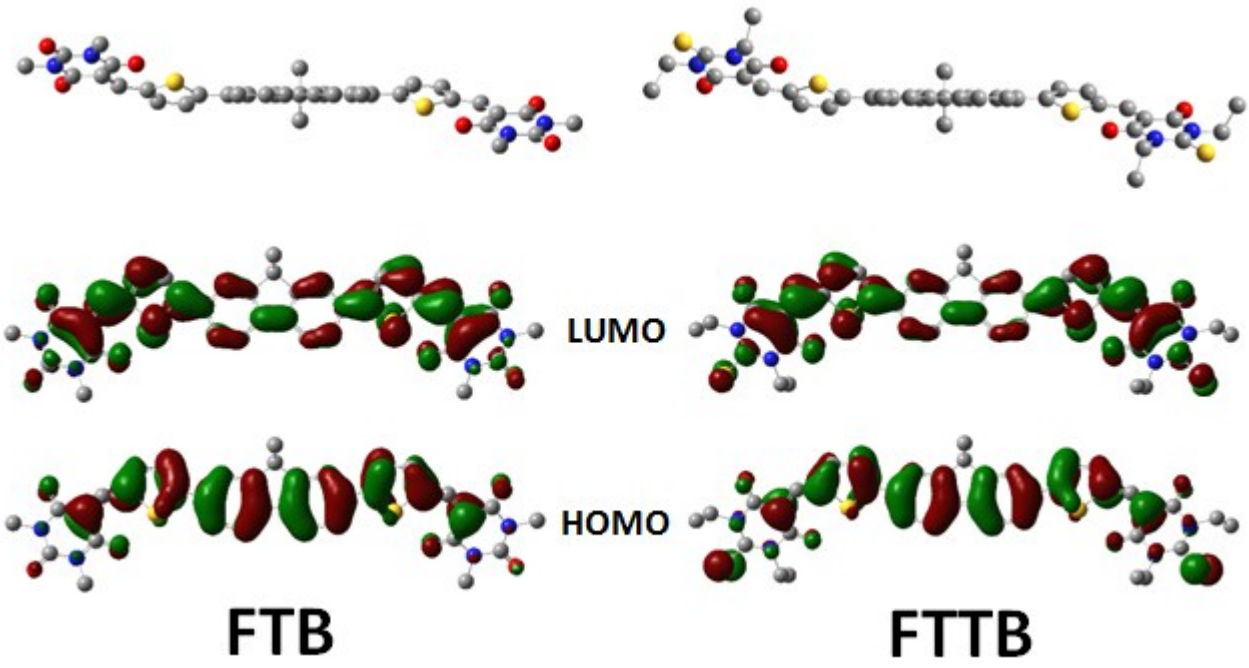

Figure S5: Minimum energy conformation of FTB and FTTB molecules calculated using Gaussian (B3LYP/6-13G*) and a visualization of their respective LUMO and HOMO distributions

Table S1: Optoelectronic properties of FTB, FTTB and PSEHTT

	ε_{max} (10^4 $M^{-1}cm^{-1}$)[a]	Film Eg_{opt} (eV)[b]	HOMO (eV)[c]	LUMO (eV)[d]
FTB	**7.71**	**2.16**	**-5.66**	**-3.50**
FTTB	**8.92**	**2.03**	**-5.75**	**-3.72**
PSEHTT	**--**	**1.84**	**-5.17**	**-3.33**

[a]Calculated from 10^{-6} M chloroform, [b]Calculated from as-cast UV-vis, [c]Calculated from film CV, [d]Calculated from HOMO + $Eg_{opt.}$

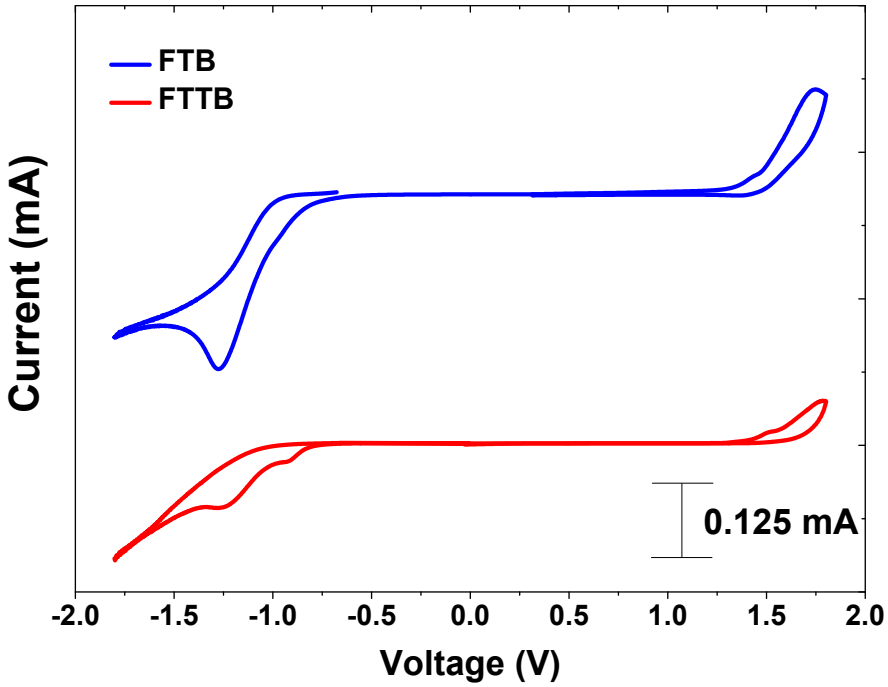

Figure S6: CV of neat FTB and FTTB films

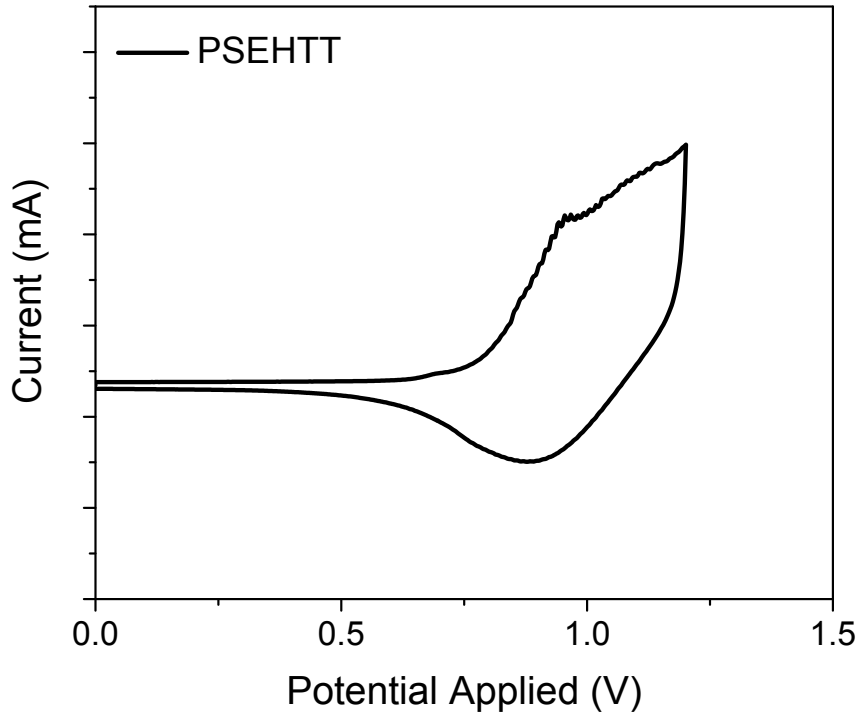

Figure S7: CV of PSEHTT film

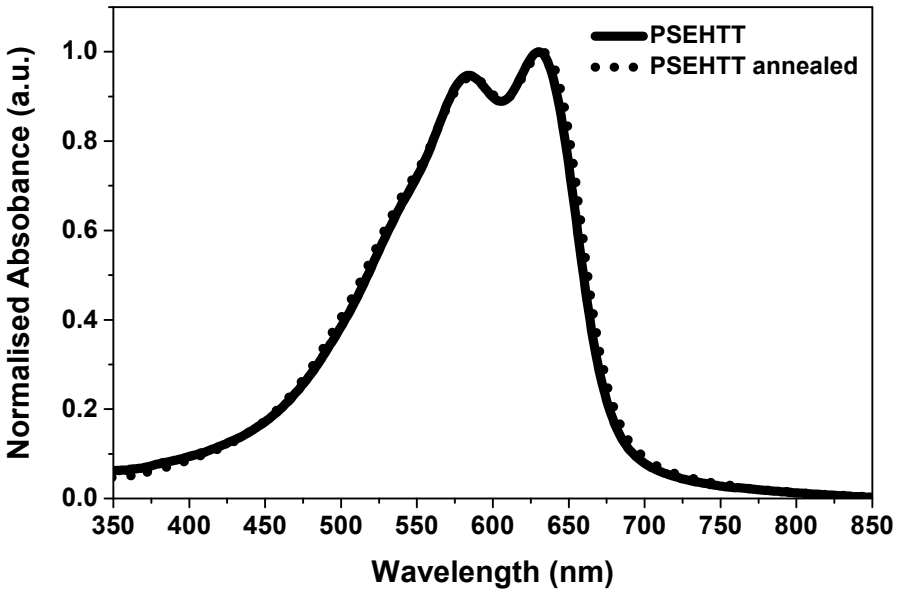

Figure S8: UV-vis absorption of neat PSEHTT film with and without annealing at 175°C for 10min

Table S2: Device optimization of PSEHTT:FTTB (1:2) with different concentrations in chlorobenzene (CB).

Blend (1:2)	**Solvent**	**Concentration (mg/mL)**	**J_{sc} ($mAcm^{-2}$)**	**V_{oc} (V)**	**FF**	**PCE (%)**
PSEHTT:FTTB	CB	8	8.13 ± 0.63	0.97 ± 0.05	0.48 ± 0.05	3.78 ± 0.73

		10	11.90 ± 0.87	1.00 ± 0.01	0.52 ± 0.02	6.17 ± 0.50
		15	7.72 ± 0.88	1.00 ± 0.01	0.46 ± 0.04	3.60 ± 0.68

Table S3: Device optimization of blends with various solvents, annealing durations/temperatures, and D:A ratio at concentration of 10mg/mL including DIO (1, 8-diiodooctane), TMB (1, 2, 4-trimethylbenzene), PN (1-phenylnapthalene), DCB (1, 3-dichlorobenzene), THN (tetralin).

PSEHTT: (10 mg/mL)	**Solvent**	**D:A**	**Anneal (10 mins.)**	**J_{sc} ($mAcm^{-2}$)**	**V_{oc} (V)**	**FF**	**PCE (PCE_{max}) (%)**
FTB	CB	1:1	--	6.76 ± 0.53	1.18 ± 0.02	0.44 ± 0.01	3.51 ± 0.32 (4.11)
			175	4.90 ± 0.94	0.96 ± 0.04	0.45 ± 0.04	2.11 ± 0.52 (2.92)
		1:2	--	8.17 ± 0.68	1.15 ± 0.04	0.52 ± 0.03	4.84 ± 0.33 (5.42)
			110	5.86 ± 1.04	1.11 ± 0.01	0.55 ± 0.00	3.54 ± 0.67 (4.22)
			140	4.77 ± 0.78	1.06 ± 0.01	0.56 ± 0.01	2.86 ± 0.48 (3.46)
			175	5.94 ± 0.55	0.94 ± 0.14	0.43 ± 0.04	2.43 ± 0.59 (3.15)
		1:3	--	6.42 ± 0.40	1.14 ± 0.01	0.55 ± 0.02	4.00 ± 0.29 (4.36)
			175	6.75 ± 0.50	0.89 ± 0.03	0.53 ± 0.06	2.67 ± 0.40 (3.58)
	CB + 3% DIO	1:2	--	0.00 ±0.00	0.00 ±0.00	0.00 ±0.00	0.00 ±0.00 (0.00)
	CB + 1% DIO		--	3.83 ± 0.48	1.08 ± 0.01	0.47 ± 0.01	1.95 ± 0.25 (2.22)
	TMB:THN		--	8.19 ± 0.79	1.16 ± 0.01	0.51 ± 0.03	4.83 ± 0.44 (5.32)
	TMB + 2.5% PN		--	6.07 ± 0.61	0.81 ± 0.12	0.40 ± 0.05	2.00 ± 0.57 (2.56)
FTTB	CB	1:1	--	9.23 ± 0.58	1.00 ± 0.00	0.50 ± 0.02	4.63 ± 0.25 (4.98)
			175	6.76 ± 0.39	0.78 ± 0.01	0.46 ± 0.01	2.42 ± 0.16 (2.59)
		1:2	--	12.47 ± 0.83	1.00 ± 0.00	0.51 ± 0.03	6.38 ± 0.44 (7.17)
			175	6.79 ± 0.44	0.75 ± 0.02	0.44 ± 0.01	2.26 ± 0.21 (2.53)
		1:3	--	8.15 ± 0.44	0.04 ± 0.01	0.47 ± 0.02	3.58 ± 0.33 (3.92)
			175	6.43 ± 0.22	0.87 ± 0.02	0.45 ± 0.02	2.56 ± 0.09 (2.67)
	CB + 3% DIO	1:2	--	5.97 ± 0.62	0.78 ± 0.02	0.36 ± 0.01	1.68 ± 0.12 (1.68)
	CB:DCB (1:1)		--	7.11 ± 0.92	0.99 ± 0.03	0.53 ± 0.05	3.72 ± 0.57 (3.75)

	CB:DCB (9:1)		--	4.43 ± 0.87	0.96 ± 0.03	0.49 ± 0.03	2.07 ± 0.41 (2.35)
	TMB:THN		--	6.68 ± 1.05	1.12 ± 0.01	0.52 ± 0.03	3.84 ± 0.55 (4.97)
	TMB + 2.5% PN		--	5.25 ± 0.78	0.94 ± 0.02	0.53 ± 0.02	2.64 ± 0.42 (2.96)

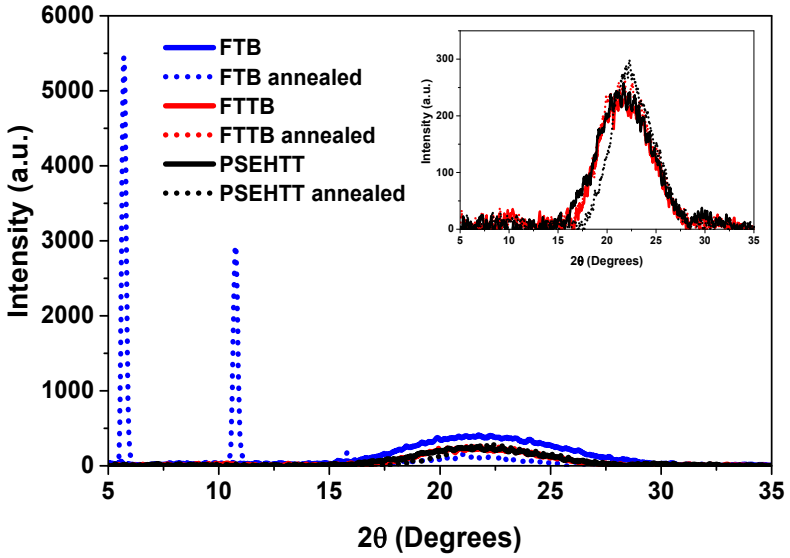

Figure S9: Drop-cast powder-XRD neat FTTB, FTB and PSEHTT films as-cast without and with annealing at 175 °C for 10 mins , inset focus on FTTB and PSEHTT at lower-intensity in the range of 15-25°

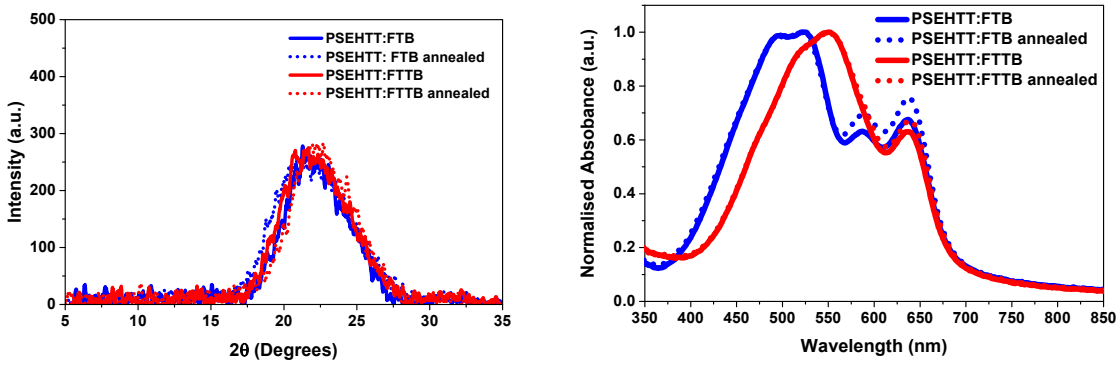

Figure S10: Drop-cast powder-XRD (left) and UV-vis absorption (right) of PSEHTT:FTB and PSEHTT:FTTB films with and without annealing at 175°C for 10 minutes

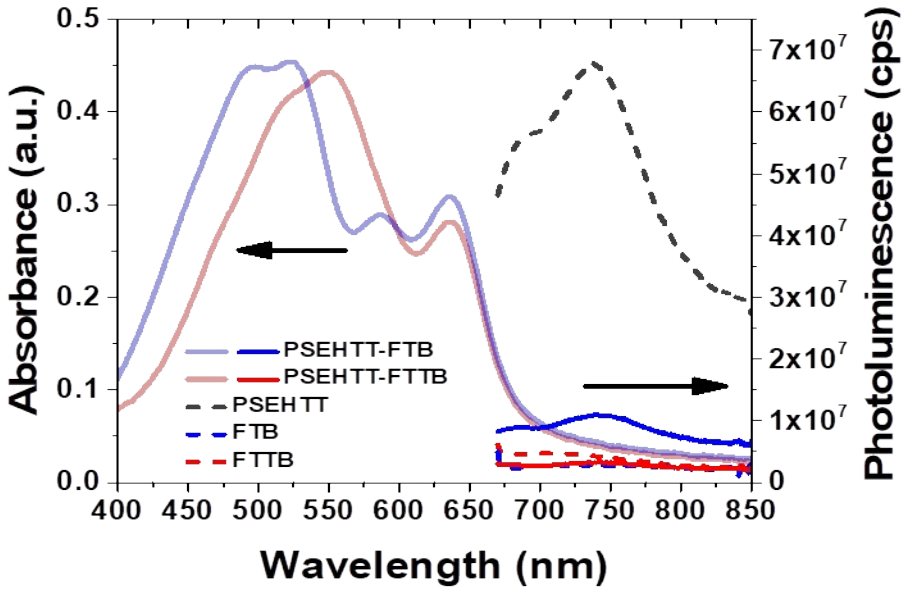

Figure S11: UV-vis absorption and photoluminescence spectra of PSEHTT:FTB and PSEHTT:FTTB blend films relative to neat PSEHTT, FTB and FTTB films employing 650 nm excitation

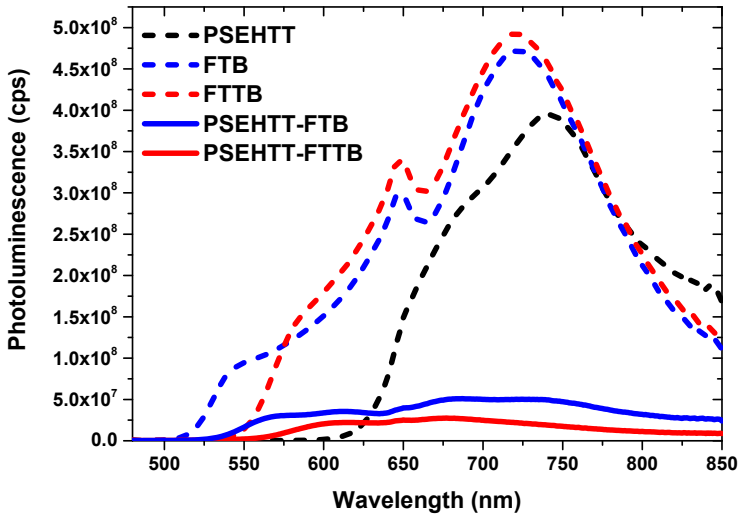

Figure S12: Photoluminescence spectra of neat PSEHTT, FTTB and FTB films and optimized recipe blends of PSEHT:FTTB and PSEHTT:FTB employing an excitation wavelength of 460nm

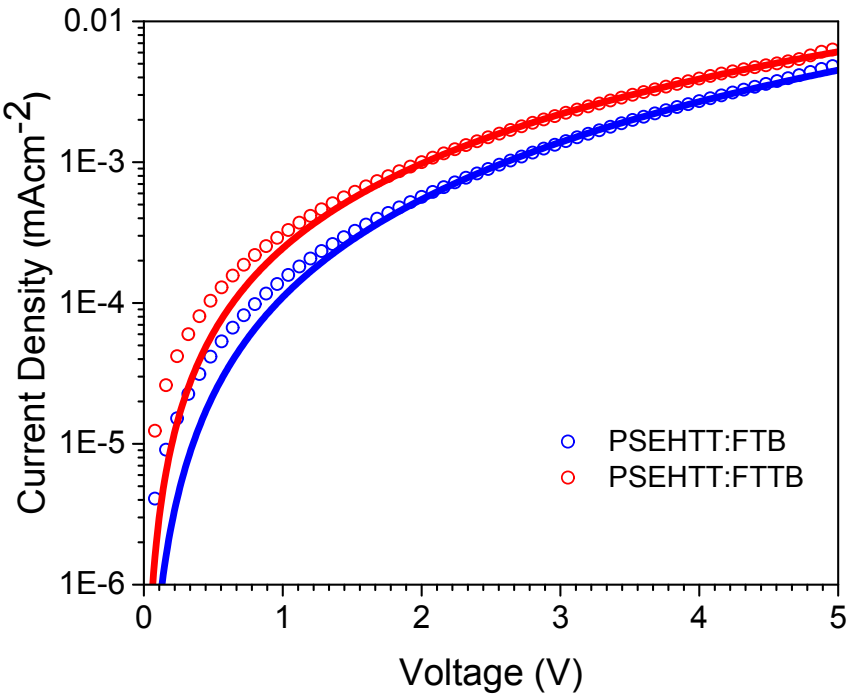

Figure S13: Hole blend change mobility (unfilled circles) and Mott-Gurney fitting (solid lines)

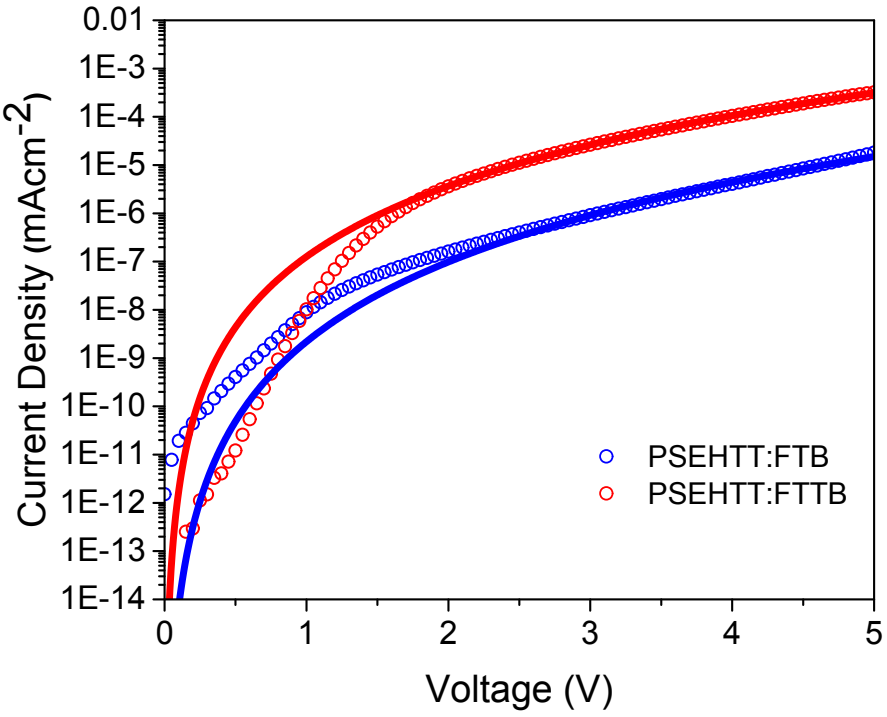

Figure S14: Electron blend change mobility (unfilled circles) and Mott-Gurney fitting (solid lines)

Table S4: Calculated electron and hole mobilities of FTB and FTTB blends and charge mobility balance.

Blend	μ_e (10^{-5} $cm^2V^{-1}s^{-1}$)	μ_h (10^{-5} $cm^2V^{-1}s^{-1}$)	μ_h/μ_e
PSEHTT:FTB	5.23 ± 0.52	7.48 ± 0.30	1.43
PSEHTT:FTTB	1.52 ± 0.10	3.48 ± 0.63	2.29

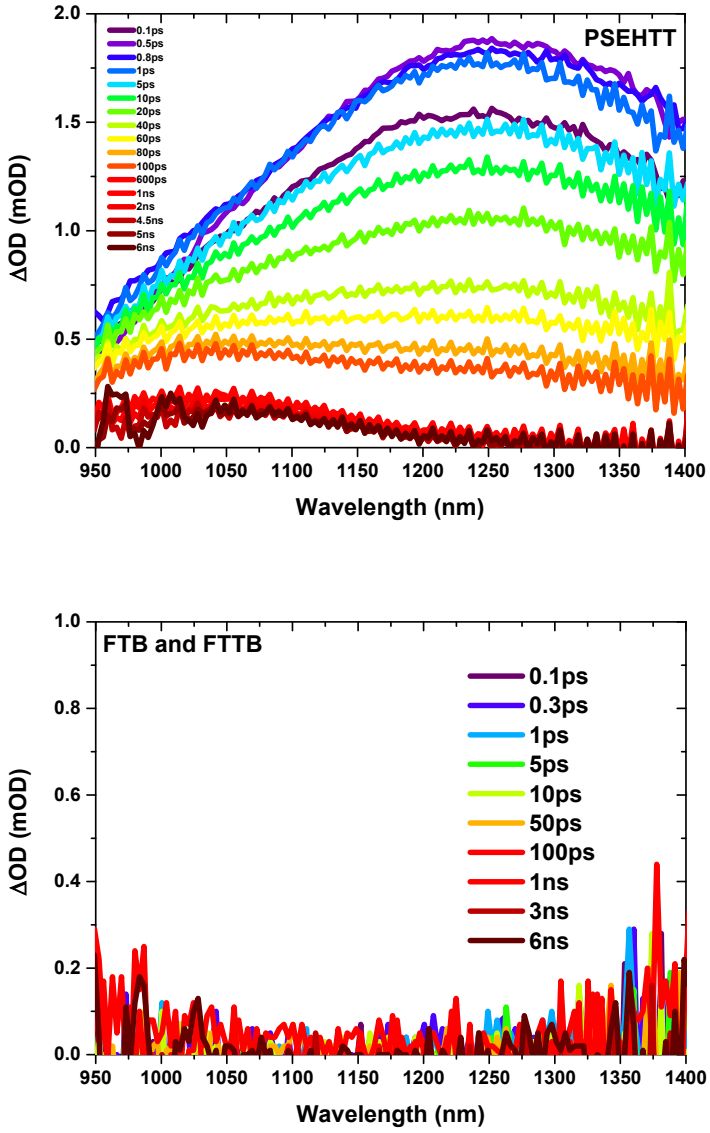

Figure S15: TA spectra of pristine PSEHTT (top) and acceptors (FTTB and FTB) (bottom) employing an excitation wavelength of 650nm and a density of 2μJ/cm^2 in N_2 atmosphere showing a sole PSEHTT exciton excitation at this wavelength

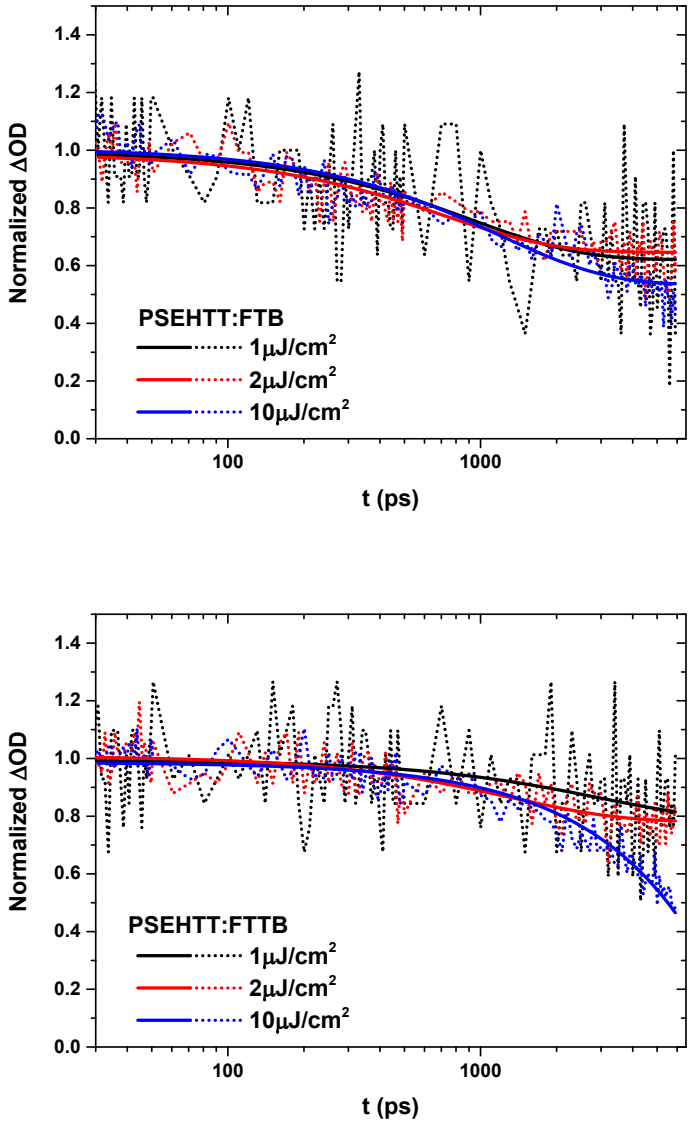

Figure S16: Kinetics probed at 1050nm (polaron) of **FTB**:PSEHTT (top) and **FTTB**:PSEHTT (bottom) films employing an excitation wavelength of 650nm and densities of 1μJ/cm^2, 2μJ/cm^2, 10μJ/cm^2 in N_2 atmosphere

References

1. A. P. Zoombelt, S. G. J. Mathijssen, M. G. R. Turbiez, M. M. Wienk and R. A. J. Janssen, *Journal of Materials Chemistry*, 2010, **20**, 2240-2246.
2. S. Y. Cho, A. C. Grimsdale, D. J. Jones, S. E. Watkins and A. B. Holmes, *Journal of the American Chemical Society*, 2007, **129**, 11910-11911.
3. K. N. Winzenberg, P. Kemppinen, F. H. Scholes, G. E. Collis, Y. Shu, T. Birendra Singh, A. Bilic, C. M. Forsyth and S. E. Watkins, *Chemical Communications*, 2013, **49**, 6307-6309.
4. E. Lim, *Bulletin of the Korean Chemical Society*, 2017, **38**, 285-288.
5. W. Ni, M. Li, B. Kan, F. Liu, X. Wan, Q. Zhang, H. Zhang, T. P. Russell and Y. Chen, *Chemical Communications*, 2016, **52**, 465-468.